Adaptive Neural Mechanism for Listing's Law Revealed in Patients with Sixth Nerve Palsy

Agnes M. F. Wong,[1,2] *Douglas Tweed,*[1,3] *and James A. Sharpe*[1,2]

Purpose. During fixation and saccades, human eye movements obey Listing's law, which specifies the torsional eye position for each combination of horizontal and vertical eye positions. To study the mechanisms that implement Listing's law, the authors measured whether the law was violated in peripheral and central unilateral sixth nerve palsy.

Methods. Twenty patients with peripheral (13 chronic, 7 acute) sixth nerve palsy, 7 patients with central sixth nerve palsy caused by brainstem lesions, and 10 normal subjects were studied with scleral search coils. With the head immobile, subjects made saccades to a target that moved between straight ahead and eight eccentric positions. At each target position, fixation was maintained for 3 seconds before the next saccade. To quantify violations of Listing's law, we measured ocular torsion during fixation and during saccades, and compared it with the torsion predicted by the law. The SD of the differences between the predicted and measured torsion was called Listing deviation.

Results. Patients with central sixth nerve palsy had abnormal ocular torsion in both the paretic and nonparetic eyes, which violated Listing's law. During fixation, Listing deviation averaged 2.4° in the paretic eye and 1.7° in the nonparetic eye, compared with 0.8° in normal control subjects ($P < 0.05$). During saccades, the Listing deviation averaged 2.7° in the paretic eye, and 1.6° in the nonparetic eye, compared with 0.8° in normal control eyes ($P < 0.05$). Donders' law was also violated in both eyes of patients with central sixth nerve palsy. They showed an abnormally wide range of ocular torsion in any given gaze direction. In contrast, patients with acute peripheral palsy had abnormal ocular torsion only in the paretic eye. Listing deviation of the paretic eye averaged 2.3° during fixation and 3.2° during saccades ($P < 0.05$). Donders' law was obeyed in acute peripheral palsy. Patients with chronic peripheral sixth nerve palsy obeyed Listing's and Donders' laws during both fixation and saccades.

Conclusions. Patients with central unilateral sixth nerve palsy have abnormal ocular torsion in both eyes, demonstrating that brainstem circuits normally participate in the maintenance of Listing's law. Eye movements in patients with acute peripheral sixth nerve palsy violate Listing's law, whereas those in patients with chronic peripheral palsy obey it, indicating that neural adaptation can restore Listing's law, even when the eye muscle remains abnormal. (*Invest Ophthalmol Vis Sci.* 2002; 43:112–119)

During fixation, saccades, and smooth pursuit, the eyes rotate freely in the horizontal and vertical dimensions, with torsion being constrained.[1–3] This constraint on torsion has been described by Donders' and Listing's laws.[4] Donders' law states that there is only one torsional eye position for each combination of horizontal and vertical eye positions.[2,4] Listing's law is a special case of Donders' law and quantitatively specifies the torsional angle for each gaze direction. It states that, with the head fixed, there is an eye position called primary position, with the property that all other eye orientations that the eye assumes can be reached by a single rotation around an axis in a plane called Listing's plane.[4]

Listing's law has been studied systematically in monkeys[5–9] and normal humans,[1,2,10,11] but not in subjects with paralytic strabismus. In the current study, we investigated patients with unilateral sixth nerve palsy to determine whether their eye movements obey Listing's law during fixation and saccades. We found that patients with central sixth nerve palsy have abnormal ocular torsion in both eyes, suggesting that brainstem circuits normally help maintain Listing's law. Eye movements in patients with acute peripheral sixth nerve palsy violate Listing's law, whereas those in patients with chronic peripheral palsy obey it, suggesting that neural adaptation can restore Listing's law even when the eye muscle remains abnormal.

Methods

We recruited 27 patients with unilateral sixth nerve palsy from the Neuro-ophthalmology Unit at the University Health Network. A complete history was taken, and detailed ophthalmic and neurologic examinations were performed. The age of onset, the presence or absence of risk factors for ischemia (diabetes mellitus and hypertension), duration of diplopia, and associated neurologic symptoms and signs were recorded. Patients with diplopia of less than 4 weeks' duration were classified as having acute palsy; all others were classified as having chronic palsy. Strabismus was measured using the prism and cover test and the Maddox rod. When indicated, appropriate tests were performed to rule out myasthenia gravis, thyroid ophthalmopathy, other orbital diseases, or intracranial lesions.

Ranges of duction were estimated by either of two examiners (AMFW, JAS) who graded the abduction defect as the estimated percentage of the normal abduction in the other eye. Based on the abduction defect, patients were classified into three groups: mild (81%–95% of normal range of abduction), moderate (51%–80%), and severe (≤50%).

Serial axial and sagittal T_1- and T_2-weighted magnetic resonance (MR) images with gadolinium enhancement were obtained (slice thickness, 5 mm) in all patients under 50 years of age and in those with other neurologic signs. In this investigation, computed tomographic (CT) images of the head with contrast were obtained in all patients with ischemic risk factors and in patients more than 50 years of age, although CT imaging is not our standard practice in such patients. If

From the [1]Division of Neurology and the Departments of [2]Ophthalmology and [3]Physiology, the University of Toronto, and University Health Network, Toronto Western Hospital, Toronto, Ontario, Canada.

Supported by the E. A. Baker Foundation, Canadian National Institute for the Blind; the Vision Science Research Program, University of Toronto; and Canadian Institutes of Health Research Grants MT 15362 and ME 5504.

Submitted for publication April 18, 2001; revised July 2, 2001; accepted July 30, 2001.

Commercial relationships policy: N.

The publication costs of this article were defrayed in part by page charge payment. This article must therefore be marked "*advertisement*" in accordance with 18 U.S.C. §1734 solely to indicate this fact.

Corresponding author: James A. Sharpe, Division of Neurology, University Health Network, EC 5-042, Toronto Western Hospital, 399 Bathurst Street, Toronto, Ontario, Canada M5T 2S8; sharpej@uhnres.utoronto.ca.

findings in CT imaging were normal, patients were followed up at approximately 3 months. Those without improvement of the sixth nerve palsy at 3 months and those with an abnormal CT scan were further investigated with MR imaging.

Eye Movement Recordings

Visual Stimuli and Experimental Protocol. Eye position was measured with search coils while patients fixated a red laser spot of 0.25° in diameter, rear projected onto a vertical, flat screen 1 m away from the nasion. The laser was programmed to appear in nine different target positions, arranged in a 3 × 3-grid square. The middle row of this array was at eye level; the other two were 10° above and below. In each row, the center target lay in the patient's midsagittal plane and the other two 10° to the right and left of it.

With one eye covered, subjects were instructed to follow the laser spot as it stepped among positions. At each position, the laser halted for 3 seconds. In the horizontal target sequence, the laser started in the center, then stepped to the 10° right position, then back to center, then 10° left, cycling through this pattern 20 times for each eye. The vertical sequence was the same but with the laser stepping center-up-center-down; the two diagonal sequences stepped along oblique lines, between opposite corners of the target array. Recordings were then made with the other eye fixating and the fellow eye occluded. Recordings were not made during binocular viewing. To avoid fatigue, breaks were provided approximately every 2 minutes for 1 to 3 minutes.

Recordings of Eye Movement and Calibration. Eye positions were measured by a three-dimensional magnetic search coil technique, using a 6-foot (183-cm) diameter coil field arranged in a cube (CNC Engineering, Seattle, WA). In each eye, the patient wore a dual-lead scleral coil annulus designed to detect horizontal, vertical, and torsional gaze positions (Skalar Instrumentation, Delft, The Netherlands). Horizontal and vertical eye movements were calibrated with saccades to steps of the laser target. Torsional movements were calibrated by attaching the scleral coil to a rotating protractor. Phase detectors using amplitude modulation as described by Robinson[12] provided signals of torsional gaze position within the linear range. Torsional precision was approximately ±0.2°. There was minimal crosstalk, and large horizontal and vertical movements produced deflections in the torsional channel of less than 4% of the amplitude of the horizontal and vertical movement. Any coil slippage was assessed by monitoring offsets in torsional eye position signal during testing. Consistency of calibrated positions after each eye movement provided evidence that the coil did not slip on the eye. Eye position data were filtered with a bandwidth of 0 to 90 Hz and digitized at 200 Hz. They were recorded on disc for off-line analysis. Analog data were also displayed in real time by a rectilinear thermal array recorder (Model TA 2000; Gould Inc., Cleveland, OH).

Coordinate System

Listing's law can be expressed using different coordinate systems.[1,10,11,13–15] In this study, we used Helmholtz's coordinate, which is particularly useful in presenting binocular data.[15] In this system, an eye position is decomposed into a series of three subrotations. Starting from primary position: first a torsional rotation through angle T around the line of sight, then a horizontal rotation through angle H around a head-fixed vertical axis, and finally a vertical rotation through angle V around the interaural axis. Expressed in Helmholtz coordinates, Listing's law says that:

$$T = -HV/2$$

where all angles are given in radians (not degrees). Positive directions for angles T, H, and V are clockwise (CW), right, and up, respectively, all from the subject's point of view. The equation is actually not precisely equivalent to Listing's law, but it is a very close approximation; within 30° of primary position, the discrepancy is less than 0.1°.[16]

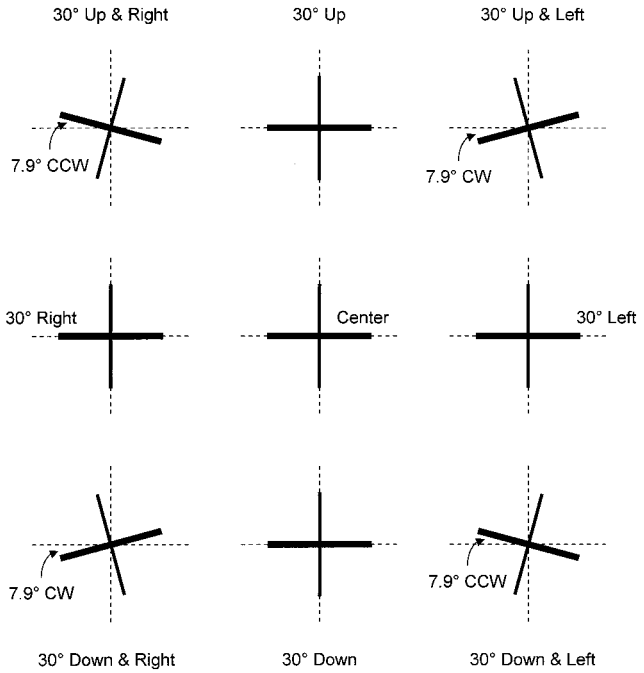

FIGURE 1. Torsional positions of the eye, as represented by the *thin lines* in relation to the vertical meridian, in different combinations of horizontal and vertical eye positions, as viewed by the examiner. If the eye is 30° down and 30° left (*bottom right panel*), then the eye rotates 7.9° (0.14 radians) CCW, in relation to the vertical meridian (*dashed line*). CW, clockwise from the subject's reference; CCW, counterclockwise from the subject's reference.

We defined the direction of torsion from the subject's point of view. Rotation of the upper pole of the iris toward the subject's right shoulder was designated as CW, whereas rotation of the upper pole of the iris toward the subject's left shoulder was designated as counterclockwise (CCW).

As the equation makes clear, Listing's law requires that the Helmholtz torsional angle of the eye vary as a function of horizontal and vertical eye position. Figure 1 depicts the torsional positions of the eye, represented by thin black lines with respect to the vertical meridian, in different combinations of horizontal and vertical eye positions, as viewed by the examiner. If the eye is 30° down and 30° left (bottom right panel), then the eye (thin black line) rotates 7.9° (0.14 radians) CCW, with respect to the vertical meridian (dashed line). In other words, Listing's law specifies quantitatively the degree of ocular torsion for any given horizontal and vertical eye position. Any torsion that differs from that specified by the equation means that Listing's law is violated.

Data Analysis and Statistical Methods

Eye position and angular velocity were computed from coil signals.[13,17] Eye positions are expressed using Helmholtz angles in degrees.[16] For analysis, fixations were defined as periods when eye velocity was less than 30°/sec, and saccades when eye velocity exceeded 50°/sec. For each subject, we computed a set of best-fit functions, expressing each eye's torsion as a function of its horizontal and vertical angles, and expressing the horizontal and vertical angles of the nonviewing eye as a function of the horizontal and vertical angles of the viewing eye. Using these fitted functions, we then computed the typical torsion of both eyes, and the typical horizontal and vertical positions of the nonviewing eye, when the viewing eye fixated the nine targets in our array. For example, Figure 2A shows the eye movement recordings of patient CS while the nonparetic left eye viewed a target that stepped as follows: center-10° up-center-10° down. Figure 2B shows the hori-

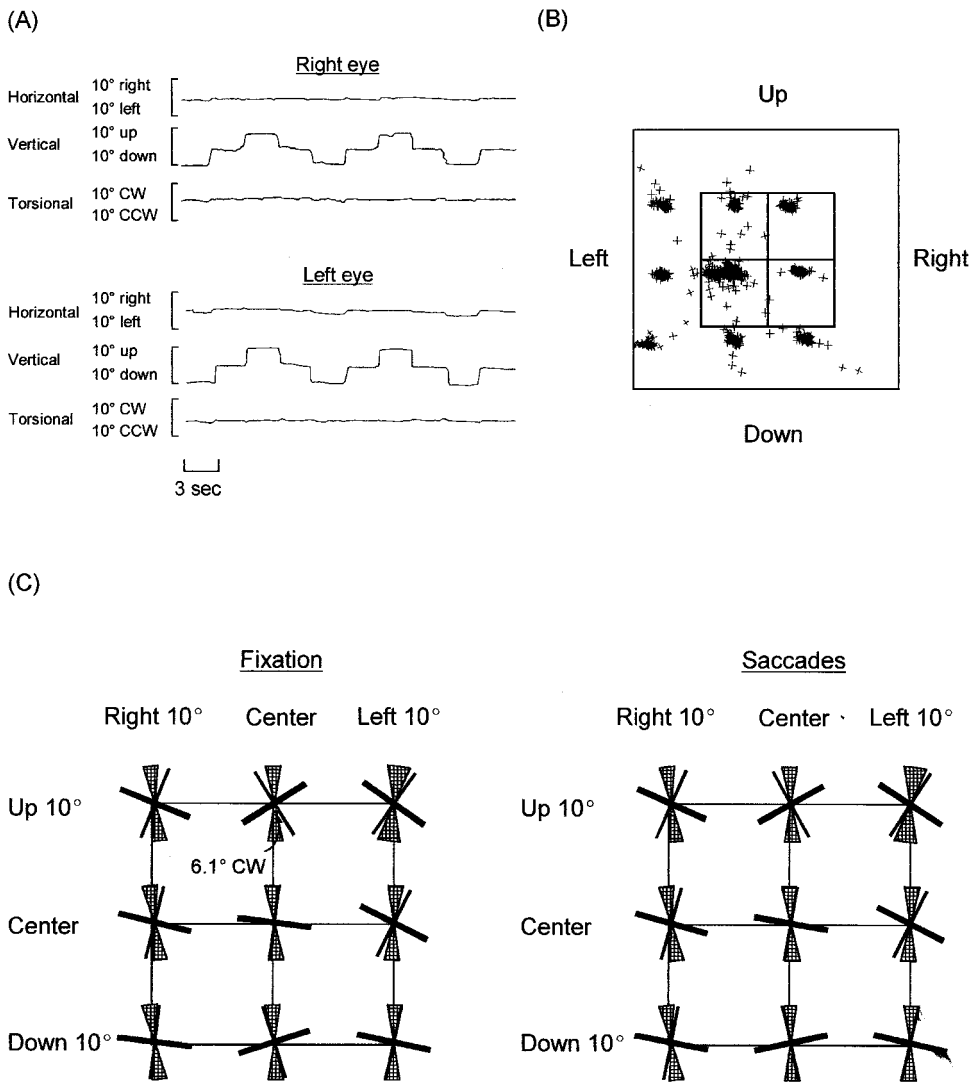

FIGURE 2. (**A**) Eye movement recordings in patient CS while the nonparetic left eye viewed a target that stepped as follows: center–10° up–center–10° down. (**B**) Horizontal, vertical, and torsional eye positions of the paretic nonviewing right eye of this patient, from the patient's viewpoint, while the left eye looked at the nine target positions—the nine corners of the black grid in the figure. The center of each small cross marks the gaze direction of the right eye. The tilt of the cross depicts the eye's torsion. We fitted functions to these data to find the typical torsion of the right eye for each position of the left. (**C**) The typical torsion of the patient's right eye in different combination of horizontal and vertical positions, shown from the examiner's viewpoint, are represented by large crosses as computed using fitted functions. For comparison, the regions with a grid pattern in this figure mark the range 1 SD above and below the mean torsion in normal subjects. For example, when this patient looked 10° up with the left eye, the paretic right eye was typically oriented 6.1° CW (from the patient's reference), well outside the range of normal torsion, indicating that Listing's law was violated in this position.

zontal, vertical, and torsional angles of the occluded, paretic right eye of this patient while the left eye looked at the nine target positions—the nine corners of the black grid in the figure. The center of each small cross marks the gaze direction of the right eye; the tilt of the cross depicts the eye's torsion. We fitted functions to these data to find the typical torsion of the occluded paretic right eye for each position of the fixating left eye. The large crosses in Figure 2C plot these fitted torsional positions. For comparison, the regions with a grid pattern mark the range one SD above and below the mean torsion in normal subjects. For example, when this patient looked 10° up with the left eye, the occluded paretic right eye was typically oriented 6.1° CW, well outside the range of normal torsion, indicating that Listing's law was violated in this position.

To quantify violations of Listing's law, we compared the ocular torsion in each recorded eye position with the torsion predicted by the law; the SD of the differences between the predicted and measured torsion was called Listing deviation. To quantify violations of Donders' law, we computed the second-order function of best fit (see the Appendix). The ocular torsion in each recorded eye position was compared with the torsion predicted by this second-order function; the SD of the differences between the predicted and measured torsion was called Donders deviation.

TABLE 1. Characteristics of Patients with Sixth Nerve Palsy Caused by a Presumed Peripheral Lesion

Patient	Age/Sex	Side of Lesion	Duration	Abduction Deficit (% Normal)	Imaging Findings	Comments
1 (TH)	77/M	Right	30 mo	60	Normal MRI	Idiopathic
2 (NR)	75/F	Right	4 mo	90	Normal MRI	Idiopathic
3 (RL)	77/F	Right	10 mo	95	Normal MRI	Idiopathic
4 (AM)	75/F	Right	2 mo	70	Normal CT	Resolved after 6 months (HTN)
5 (GD)	64/M	Right	15 mo	90	Normal CT	Claustrophobia
6 (KE)	75/F	Right	2 mo	10	Normal CT	Resolved after 4 months (HTN, DM)
7 (TH)	57/M	Right	2 mo	90	Normal CT	Resolved after 4 months (HTN, DM)
8 (DW)	65/M	Left	96 mo	70	Normal MRI	Idiopathic
9 (GC)	57/M	Left	34 mo	90	Normal MRI	Idiopathic
10 (VI)	65/F	Left	36 mo	50	Normal MRI	Idiopathic
11 (SCH)	50/F	Left	24 mo	80	Normal MRI	Idiopathic
12 (IW)	75/F	Left	12 mo	90	Normal MRI	Idiopathic
13 (LC)	54/F	Left	60 mo	80	Normal MRI	Idiopathic
14 (PL)	21/M	Right	2 wk	0	Normal MRI	Improved after 4 months
15 (JM)	46/M	Right	2 wk	0	Normal MRI	Resolved after 3 months
16 (EF)	52/M	Right	3 wk	95	Normal MRI	Idiopathic
17 (SC)	66/M	Right	3 wk	80	Normal CT	Resolved after 4 months (DM)
18 (JM2)	46/M	Left	3 wk	80	Normal MRI	Resolved after 6 months (HTN)
19 (EM)	64/M	Left	3 wk	80	Normal CT	Resolved after 5 months (HTN)
20 (MB)	19/F	Left	3 wk	0	MRI: left cavernous sinus hemangioma	Botulin injection at 3 months

HTN, hypertension; DM, diabetes mellitus.

In all 27 patients, Listing and Donders deviations in both the paretic and nonparetic eyes did not differ during paretic or nonparetic eye viewing. In the Results section, we report only Listing and Donders deviations during nonparetic eye viewing. Deviations during paretic eye viewing were similar. Statistical analysis was performed using analysis of variance. Deviations were defined as significant when $P < 0.05$.

The research protocol was approved by the University Health Network Ethics Committee and followed the tenets of the Declaration of Helsinki. Informed consent was obtained from all subjects.

RESULTS

General Characteristics of Patients

The characteristics of the 27 patients are shown in Tables 1 and 2. The mean age was 60 ± 15 years (median age, 64; range, 21–79); 14 were men. The duration of symptoms ranged from 1 week to 240 months, with a mean duration of 31 months. Mean follow-up duration was 13 months (range, 8–24). All patients had an incomitant esotropia, which increased in the field of action of the paretic muscle. Twenty patients had sixth nerve palsy caused by idiopathic, presumed ischemic, peripheral lesions (Table 1). Thirteen of them had chronic peripheral palsy, and seven had acute peripheral palsy. Fourteen patients had normal MR images and six had normal findings in CT scans of the brain. Five of the six patients with normal CT scan had ischemic factors, such as hypertension and diabetes and had a complete resolution of the palsy within 4 to 6 months. Seven patients had central sixth nerve palsy caused by brainstem lesions, as shown by MR imaging (Table 2). Lesions included demyelination (three patients), cavernous hemangioma (two), meningioma (one), and infarct (one). All seven patients had neurologic symptoms and signs in addition to diplopia.

Ten normal subjects served as control subjects (five women; mean age, 49 ± 12 years; median, 55; range, 19–69).

TABLE 2. Characteristics of Patients with Sixth Nerve Palsy Caused by a Central Lesion in the Brain Stem

Patient	Age/Sex	Side of Lesion	Duration	Abduction Deficit (% Normal)	Imaging Findings	Symptoms at Examination
21 (CS)	79/F	Right	19 mo	0	MRI: right pontine meningioma	Diplopia, right facial paraesthesia
22 (AK)	75/M	Right	1 wk	70	MRI: right pontine demyelinating lesion	Diplopia, ataxia (MS for 27 years)
23 (MD)	75/M	Left	240 mo	40	MRI: left caudal pontine infarct	Dysarthria, tinnitus, limb weakness
24 (WS)	59/M	Left	52 mo	90	MRI: left pontomedullary cavernoma and hematoma	Headache, right paraesthesia, ataxia
25 (RC)	56/F	Left	132 mo	70	MRI: left pontomedullary cavernoma and hematoma	Left facial palsy and paraesthesia
26 (JP)	36/F	Left	3 mo	80	MRI: left pontomedullary and middle cerebellar peduncle demyelinating lesions	Diplopia, right leg paraesthesia, ataxia
27 (WR)	30/F	Left	2 wk	70	MRI: left pontomedullary demyelinating lesion	Diplopia, ataxia

MS, multiple sclerosis.

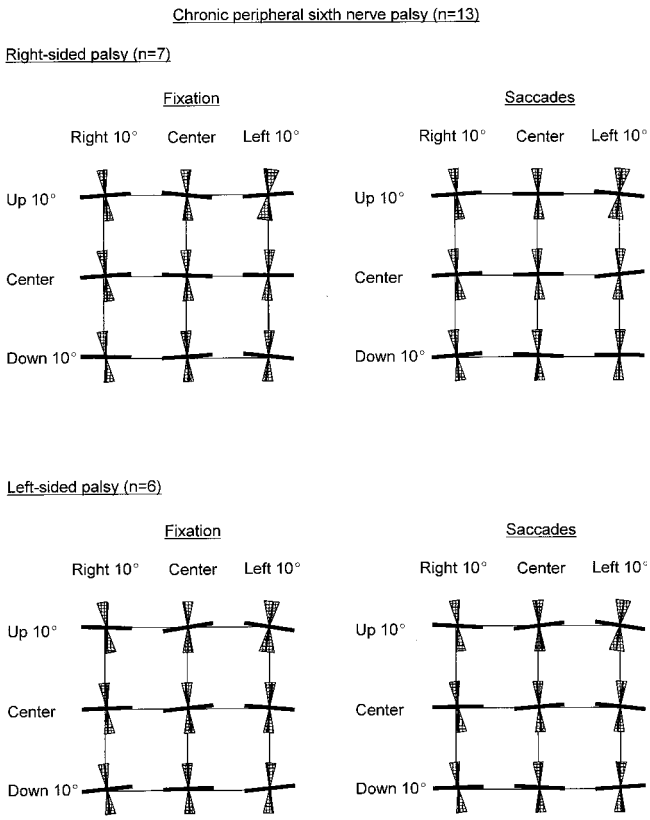

FIGURE 3. Mean torsional positions (*large crosses*) of the occluded paretic eye in nine target positions during fixation and saccades in 13 patients with chronic peripheral sixth nerve palsy, compared with the range 1 SD above and below the mean torsion in normal subjects (regions with a grid pattern). Torsional angles depicted in the figure are the actual torsional angles multiplied by five to facilitate easier viewing.

Listing and Donders Deviations in Peripheral Sixth Nerve Palsy

Chronic Peripheral Palsy. Figure 3 shows the mean torsion of the occluded paretic eye in nine target positions in patients with chronic peripheral sixth nerve palsy, compared with the range 1 SD above and below the mean torsion in normal subjects. All 13 patients had normal torsion in all nine target positions in both the paretic and nonparetic eyes, regardless of whether they had mild, moderate, or severe palsy. Listing deviation of the paretic eye averaged 0.8 ± 0.2° during fixation and 0.9 ± 0.2° during saccades, compared with 0.8 ± 0.3° in control eyes during both tasks (Fig. 4). Eye movements in chronic peripheral sixth nerve palsy obeyed Listing's law.

Acute Peripheral Palsy. Patients with acute peripheral sixth nerve palsy had abnormal torsion in the paretic eye, but normal torsion in the nonparetic eye, regardless of the severity of the palsy (Fig. 5). Listing deviation of the paretic eye averaged 2.3 ± 1.3° during fixation and 3.2 ± 2.0° during saccades (Fig. 4). Listing's law failed idiosyncratically in any of the nine target positions, with no pattern across patients.

However, eye movements in all patients with acute peripheral palsy obeyed Donders' law. Donders deviation of the paretic eye averaged 0.9 ± 0.6° during fixation compared with 0.5 ± 0.3° in normal eyes (Fig. 6). During saccades, Donders deviation averaged 0.9 ± 0.4° in the paretic eye compared with 0.6 ± 0.2° in normal control eyes (Fig. 6).

Listings and Donders Deviations in Central Sixth Nerve Palsy

Whereas patients with acute peripheral palsy had abnormal torsion only in the paretic eye, all patients with central palsy caused by brainstem lesions had abnormal ocular torsion in both eyes, regardless of the duration and severity of the palsy (Fig. 7). During fixation, Listing deviation averaged 2.4 ± 1.2° in the paretic eye and 1.7 ± 0.3° in the nonparetic eye ($P < 0.05$; Fig. 4). During saccades, Listing deviation averaged 2.7 ± 1.4° in the paretic eye and 1.6 ± 0.4° in the nonparetic eye ($P < 0.05$; Fig. 4).

Eye movements in patients with central palsy also violated Donders' law—that is, there was not one consistent angle of torsion for any given gaze direction, but rather an abnormally wide range of torsional angles. During fixation, Donders deviation averaged 1.4 ± 0.7° in the paretic eye and 1.2 ± 0.3° in the nonparetic eye ($P < 0.05$; Fig. 6). During saccades, Donders deviation averaged 1.5 ± 0.6° and 1.2 ± 0.6° in the nonparetic eye ($P < 0.05$; Fig. 6). Listing's and Donders' laws failed, not only when the target was in the paretic hemifield, but also in any one of the nine target positions.

DISCUSSION

Listing's law holds during fixation, saccades, and smooth pursuit, but fails during sleep[7,18] and vestibulo-ocular reflex (VOR).[19] Its failure shows that the eye muscles are capable of violating Listing's law, and therefore it is not the muscles but the neural commands driving fixation, saccades, and pursuit that constrain the eye to obey the law.[2,20] The muscles may, however, be arranged in a way that simplifies the brain's work in implementing Listing's law,[21–27] as in the active-pulley hypothesis,[26] which states that contraction of the global layer of

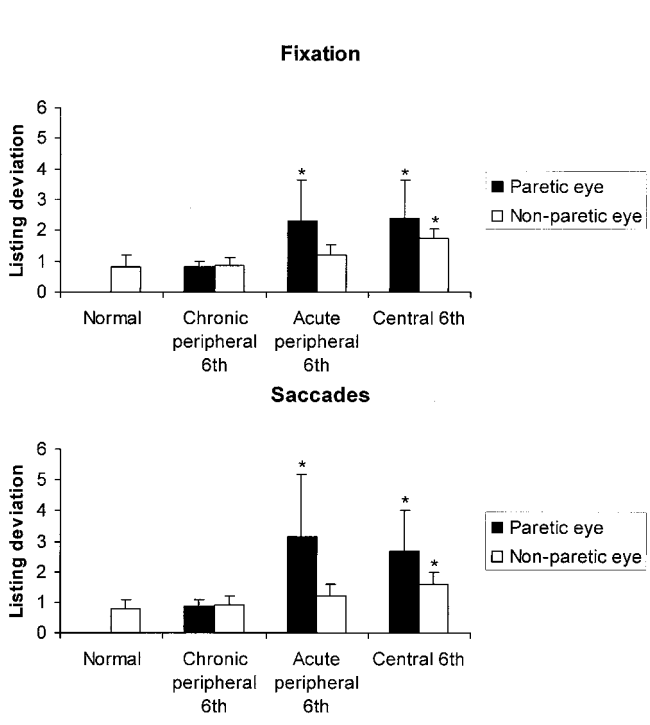

FIGURE 4. Listing deviations during fixation and saccades in normal control eyes and eyes of patients with peripheral (chronic and acute) and central sixth nerve palsy caused by brainstem lesions. *Significantly different from normal eyes, $P < 0.05$.

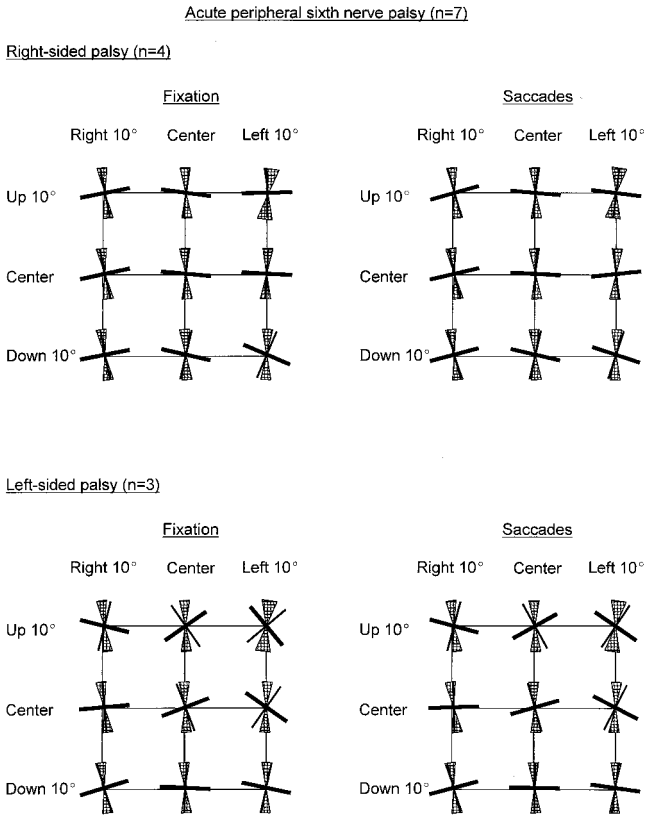

FIGURE 5. Mean torsional position (*large crosses*) of the occluded paretic eye during fixation and saccades in seven patients with acute peripheral sixth nerve palsy, compared with the range 1 SD above and below the mean torsion in normal subjects (regions with a grid pattern). Torsional angles depicted in the figure are the actual torsional angles multiplied by five to facilitate easier viewing.

the rectus muscle rotates the globe, while contraction of the orbital layer displaces the connective-tissue sleeves, or pulleys, which direct the paths of the muscles.

Active Neural Implementation of Listing's Law

In our patients with acute peripheral sixth nerve palsy, Listing's law was violated in the paretic eye, presumably because the lateral rectus muscle was paretic and perhaps also because its pulley was abnormally positioned. In patients with chronic peripheral palsy, movements in both eyes obeyed Listing's law, even though the lateral rectus was still markedly weak. This recovery shows that the neural circuitry underlying Listing's law is adaptive, restoring the law despite a palsied muscle and possibly a disrupted pulley system. Neural adaptation must work by readjusting the innervations to the remaining extraocular muscles. It may also adjust their pulleys, although, theoretically, Listing's law could be restored with or without a new pattern of pulley placement and motion. All patients with central palsy caused by brainstem lesions had abnormal ocular torsion in both the paretic and nonparetic eyes, regardless of the duration and severity of the palsy. Evidently, the neural adaptive mechanisms underlying Listing's law cannot restore it after certain brainstem lesions.

Neural Pathway for the Implementation of Listing's Law

Our results indicate that an adaptive neural mechanism is responsible for the implementation of Listing's law. However, the brain circuits responsible have not been located. A major neural pathway underlying saccadic eye movements involves the superior colliculus,[28–30] which sends saccadic signals to the medium-lead burst neurons in the pontine paramedian reticular formation (PPRF) and the rostral interstitial nucleus of the medial longitudinal fasciculus (riMLF).[31,32] These burst neurons, in turn, project to the extraocular motoneurons, the final common pathway for all eye movements.[31,32] Electrical stimulation and three-dimensional recordings in alert monkeys have shown that the superior colliculus generates saccades that fit Listing's law.[33] Stimulation of the medium-lead burst neurons in the caudal PPRF and riMLF evokes abnormal saccades that violate Listing's law.[34] These findings suggest that the circuitry implementing Listing's law is downstream from the superior colliculus and upstream from the medium-lead burst neurons.

The caudal nucleus reticularis tegmenti pontis (cNRTP), which lies ventral to the rostral PPRF, receives inputs from the superior colliculus and projects to the dorsal vermis and caudal fastigial nucleus.[35,36] Inactivation of the cNRTP causes torsional errors, indicating that the cNRTP contributes to stabilization of Listing's plane against torsional errors of the saccadic system.[37] Torsional pulsion of vertical and horizontal saccades is observed in patients with lateral medullary infarction, suggesting that the lateral medulla participates in torsional control.[38] Another center for three dimensional eye control may be in the cerebellum.[33] The influence of the NRTP on the three-dimensional control of eye movements may depend on its cerebellar projections.[39] In this study, we found that eye movements in patients with sixth nerve palsy caused by pontomedullary lesions violate Listing's law. This provides evi-

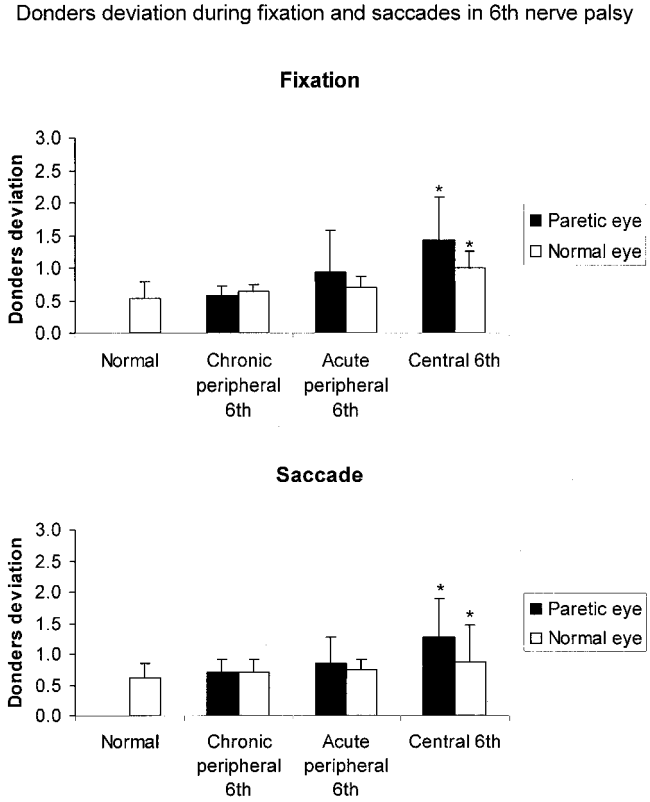

FIGURE 6. Donders deviation during fixation and saccades in normal control eyes and eyes of patients with peripheral (chronic and acute) and central sixth nerve palsy caused by brainstem lesions. *Significantly different from normal, $P < 0.05$.

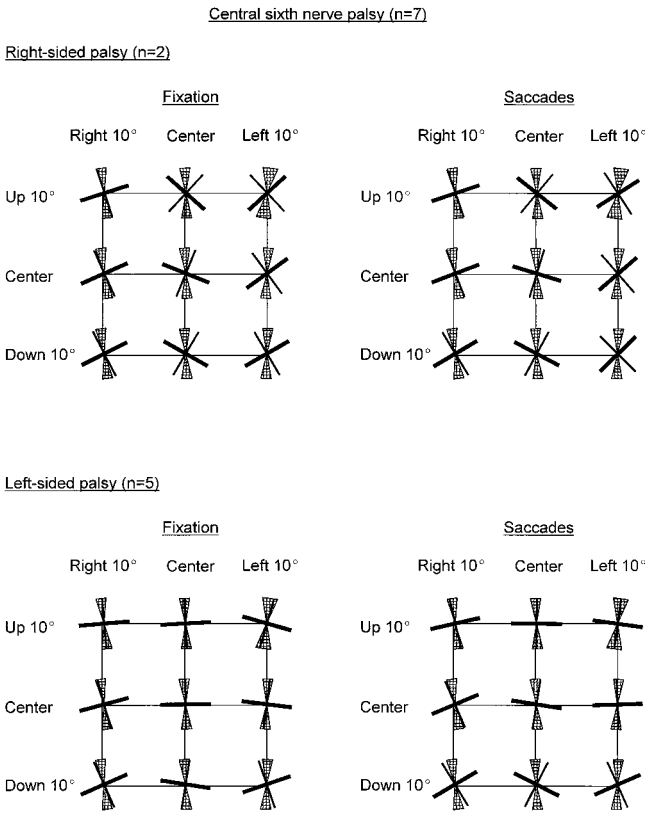

FIGURE 7. Mean torsional position (*large crosses*) of the occluded paretic eye during fixation and saccades in seven patients with central sixth nerve palsy caused by brainstem lesions, compared with the range 1 SD above and below the mean torsion in normal subjects (regions with a grid pattern). Torsional angles depicted in the figure are the actual torsional angles multiplied by five to facilitate easier viewing.

dence that this region is an element of the neural pathway that enforces Listing's law.

References

1. Tweed D, Fetter M, Andreadaki S, Koenig E, Dichgans J. Three-dimensional properties of human pursuit eye movements. *Vision Res.* 1992;32:1225–1238.
2. Tweed D, Vilis T. Geometric relations of eye position and velocity vectors during saccades. *Vision Res.* 1990;30:111–127.
3. Minken AWH, Van Opstal AJ, Van Gisbergen JAM. Three-dimensional analysis of strongly curved saccades elicited by double-step stimuli. *Exp Brain Res.* 1993;93:521–533.
4. Helmholtz Hv. *Handbuch der physiologischen Optik*. 3rd ed. Hamburg: Voss; 1867. Translated into English by Southall JPC as *Helmholtz's Treatise on Physiological Optics*. Rochester, NY: Optical Society of America; 1925:37–126.
5. Haslwanter T, Straumann D, Hepp K, Hess BJM, Henn V. Smooth pursuit eye movements obey Listing's law in the monkey. *Exp Brain Res.* 1991;87:470–472.
6. Suzuki Y, Straumann D, Hess BJM, Henn V. Changes of Listing's plane under physiological and pathological conditions. In: Delgado-Garcia JM, Godaux E, Vidal P-P, eds. *Information Processing Underlying Gaze Control*. Oxford: Pergamon Press; 1994:75–86.
7. Suzuki Y, Büttner-Ennever JA, Straumann D, et al. Deficits in vertical and torsional rapid eye movements and shift of Listing's plane after uni- and bilateral lesions of the rostral interstitial nucleus of the medial longitudinal fasciculus (riMLF). *Exp Brain Res.* 1995;106:215–232.
8. Suzuki Y, Kase M, Kato H, Fukushima K. Stability of ocular counterrolling and Listing's plane during static roll-tilts. *Invest Ophthalmol Vis Sci.* 1997;38:2103–2111.
9. Helmchen C, Rambold H, Fuhry L, Büttner U. Deficits in vertical and torsional eye movements after uni- and bilateral muscimol inactivation of the interstitial nucleus of Cajal of the alert monkey. *Exp Brain Res.* 1998;119:436–452.
10. Ferman L, Collewijn H, Berg AV. A direct test of Listing's law. I: human ocular torsion measured in static tertiary position. *Vision Res.* 1987;27:929–928.
11. Ferman L, Collewijn H, Berg AV. A direct test of Listing's law, II: human ocular torsion measured under dynamic conditions. *Vision Res.* 1987;27:939.
12. Robinson DA. A method of measuring eye movement using a scleral search coil in a magnetic field. *IEEE Trans Biomed Electron.* 1963;10:137–144.
13. Tweed D, Vilis T. Implications of rotational kinematics for the oculomotor system in three dimensions. *J Neurophysiol.* 1987;58:832–849.
14. Haustein W. Considerations on Listing's law and the primary position by means of a matrix description of eye position control. *Biol Cybern.* 1989;60:411–420.
15. Somani RAB, DeSouza JFX, Tweed D, Vilis T. Visual testing of Listing's law during vergence. *Vision Res.* 1998;38:911–923.
16. Tweed D. Visual-motor optimization in binocular control. *Vision Res.* 1997;37:1939–1951.
17. Tweed D, Cadera W, Vilis T. Computing three-dimensional eye position quaternions and eye velocity from search coil signals. *Vision Res.* 1990;30:97–110.
18. Nakayama K. Coordination of extraocular muscles. In: Lennerstrand G, Bach-y-Rita P, eds. *Basic Mechanisms in Ocular Motility and Their Clinical Applications.* New York: Pergamon Press; 1975:193–207.
19. Tweed D, Sievering D, Misslisch H, Fetter M, Zee D, Koenig E. Rotational kinematics of the human vestibuloocular reflex. III: Listing's law. *J Neurophysiol.* 1994;72:2490–2502.
20. Crawford JD, Vilis T. How do motor systems deal with the problem of controlling three-dimensional rotations? *J Motor Behav.* 1995;27:89–99.
21. Schnabolk C, Raphan T. Modeling three-dimensional velocity-to-position transformation in oculomotor control. *J Neurophysiol.* 1994;71:623–638.
22. Demer JL, Miller JM, Poukens V, Vinters HV, Glasgow BJ. Evidence for fibromuscular pulleys of the recti extraocular muscles. *Invest Ophthalmol Vis Sci.* 1995;36:1125–1136.
23. Straumann D, Zee DS, Solomon D, Lasker AG, Roberts DC. Transient torsion during and after saccades. *Vision Res.* 1995;35:3321–3334.
24. Quaia C, Optican LM. Commutative saccadic generator is sufficient to control a 3-D ocular plant with pulleys. *J Neurophysiol.* 1998;79:3197–3215.
25. Raphan T. Modeling control of eye orientation in three dimensions. I: role of muscle pulleys in determining saccade trajectory. *J Neurophysiol.* 1998;79:2653–2667.
26. Demer JL, Oh SY, Poukens V. Evidence of active control of rectus extraocular muscle pulleys. *Invest Ophthalmol Vis Sci.* 2000;41:1280–1290.
27. Thurtell MJ, Kunin M, Raphan T. Role of muscle pulleys in producing eye position-dependence in the angular vestibuloocular reflex: a model-based study. *J Neurophysiol.* 2000;84:639–650.
28. Lee C, Rohrer WH, Sparks DL. Population coding of saccadic eye movements by neurons in the superior colliculus. *Nature.* 1988;332:357–360.
29. Waitzman DM, Munoz DP, Optican LM, Wurtz RH. Saccade-related burst cells of the superior colliculus are modulated by electrical stimulation of its rostral pole. *Soc Neurosci Abstr.* 1990;16:1084.
30. Waitzman DM, Ma TP, Optican LM, Wurtz RH. Superior colliculus neurons mediate the dynamic characteristics of saccades. *J Neurophysiol.* 1991;66:1716–1737.
31. Hepp K, Henn V, Vilis T, Cohen B. Brainstem regions related to saccade generation. In: Wurtz RH, Goldberg ME, eds. *The Neurobiology of Saccadic Eye Movements.* Amsterdam: Elsevier; 1989:105–212.
32. Fuchs AF, Kaneko CRS, Scudder CA. Brainstem control of saccadic eye movements. *Annu Rev Neurosci.* 1985;8:307–337.

33. Hepp K, Van Opstal AJ, Straumann D, Hess BJM, Henn V. Monkey superior colliculus represents rapid eye movements in a two-dimensional motor map. *J Neurophysiol.* 1993;69:965–979.
34. Hepp K, Suzuki J, Straumann D, Hess BJM. On the 3-dimensional rapid eye movement generator in the monkey. In: Delgado-Garcia JM, Godeaux E, Vidal PP, eds. *Information Processing Underlying Gaze Control.* Oxford: Pergamon Press; 1995:65–74.
35. Gerrits NM, Voogd J. The nucleus reticularis tegmenti pontis and the adjacent rostral paramedian reticular formation: differential projections to the cerebellum and the caudal brainstem. *Exp Brain Res.* 1986;62:29–45.
36. Noda H, Sugita S, Ikeda Y. Afferent and efferent connections of the oculomotor region of the fastigial nucleus in the macaque monkey. *J Comp Neurol.* 1990;302:330–348.
37. Van Opstal J, Hepp K, Suzuki Y, Henn V. Role of monkey nucleus reticularis tegmenti pontis in the stabilization of Listing's plane. *J Neurosci.* 1996;16:7284–7296.
38. Morrow MJ, Sharpe JA. Torsional nystagmus in the lateral medullary syndrome. *Ann Neurol.* 1988;24:390–398.
39. Siebold C, Glonti L, Kleine J, Büttner U. Saccade-related activity in the fastigial nucleus of the monkey during 3-D eye movements. *Soc Neurosci Abstr.* 1997;23:1298.

APPENDIX

To quantify how well eye movements in the participants obeyed Listing's law, we computed the best-fit function relating the eye's torsion (t) to its horizontal and vertical angles, (h) and (v), in a three-parameter equation

$$t = -hv/2 + a_1 + a_2h \cdot a_3v$$

We computed the parameters a_1 through a_3 that yielded the best fit to the data, where a_1 quantifies any torsional shift of primary position and a_2 and a_3 quantify its vertical and horizontal rotation. This equation defined a surface of best fit to the eye-position data. The SD of the separation of the data points from the surface was Listing deviation.

To quantify adherence to Donders' law, we fitted a very flexible, curved surface to the same eye-position data using a 15-parameter equation

$$t = a_1 + a_2h + a_3v + a_4d_h + a_5d_v + a_6h^2 + a_7hv + a_8hd_h + a_9hd_v + a_{10}v^2 + a_{11}vd_h + a_{12}vd_v + a_{13}d_h^2 + a_{14}d_hd_v + a_{15}d_v^2$$

where d_h is disconjugate horizontal eye position (i.e., the difference between the Helmholtz horizontal angles of the two eyes) and d_v is disconjugate vertical eye position. The SD of the data points' separation from this surface we called Donders deviation, reasoning that, if the data could not be well fitted using a highly flexible surface with 15 parameters, they were probably not confined to any surface at all.